Supplementary Information

Supplementary Fig. 1. Opposing effects of HCoV-229E or MERS-CoV on ER stress genes at the mRNA and protein level.

Supplementary Fig. 2. PERK inhibition by GSK2656157 suppresses CoV replication.

Supplementary Fig. 3. Thapsigargin suppresses MERS-CoV and SARS-CoV-2 N protein and upregulates BiP in infected cells.

Supplementary Fig. 4. Thapsigargin suppresses Influenza A virus but not poliovirus replication.

Supplementary Fig. 5. Comparison of the antiviral effects of thapsigargin and remdesivir.

Supplementary Fig. 6. Identification of deregulated cellular pathways in MERS-CoV-infected HuH7 cells.

Supplementary Fig. 7. Identification of deregulated cellular pathways in SARS-CoV-2-infected Vero E6 cells.

Supplementary Fig. 8. Top pathways regulated by MERS-CoV, SARS-CoV-2 or thapsigargin.

Supplementary Fig. 9. Projection of thapsigargin effects on protein levels of pathway KEGG hsa04141.

Supplementary Fig. 10. Effects of bafilomycin A_1 on the viability of HCoV-229E-infected and thapsigargin-treated HuH7 cells.

Supplementary Fig. 11. Analysis of inflammatory host cell transcripts showing thapsigargin-independent uncoupling of mRNA and protein levels in HCoV-229E-infected cells.

Supplementary Table 1. List of all commercial Taqman assays and primers used in this study.

HCoV-229E / - (24 h)

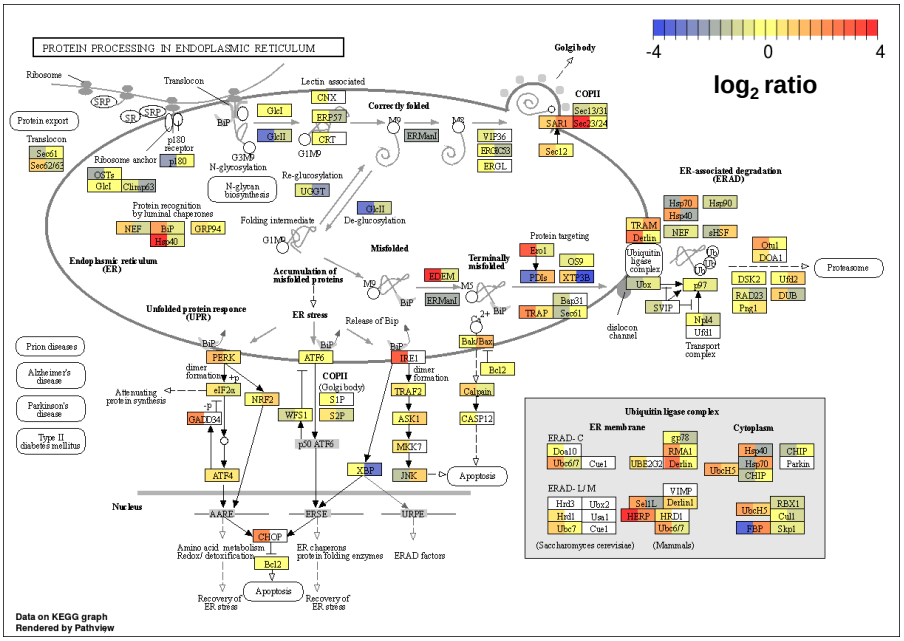

MERS-CoV / - (24 h)

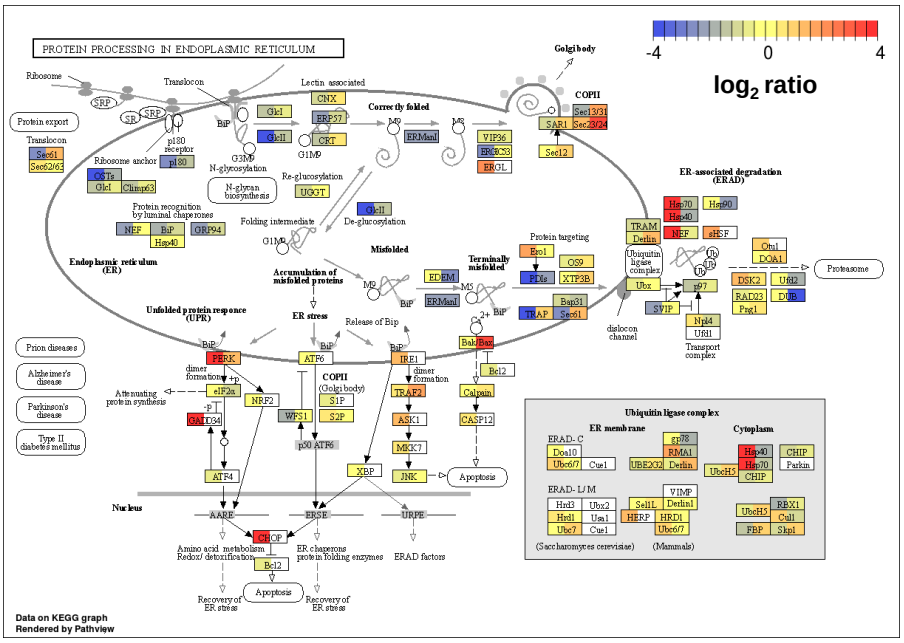

Supplementary Fig. 1. Opposing effects of HCoV-229E or MERS-CoV on ER stress genes at the mRNA and protein level.

Projection of ratio values obtained from normalized transcriptomic (by RNA-seq) and proteomic (by LC-MS/MS) data derived in parallel from HuH7 cells infected for 24 h with HCoV-229E or MERS-CoV with a MOI=1 on the components of the KEGG pathway hsa04141 “protein processing in endoplasmic reticulum”. The left side of the boxes show mRNA values, right sides show protein values.

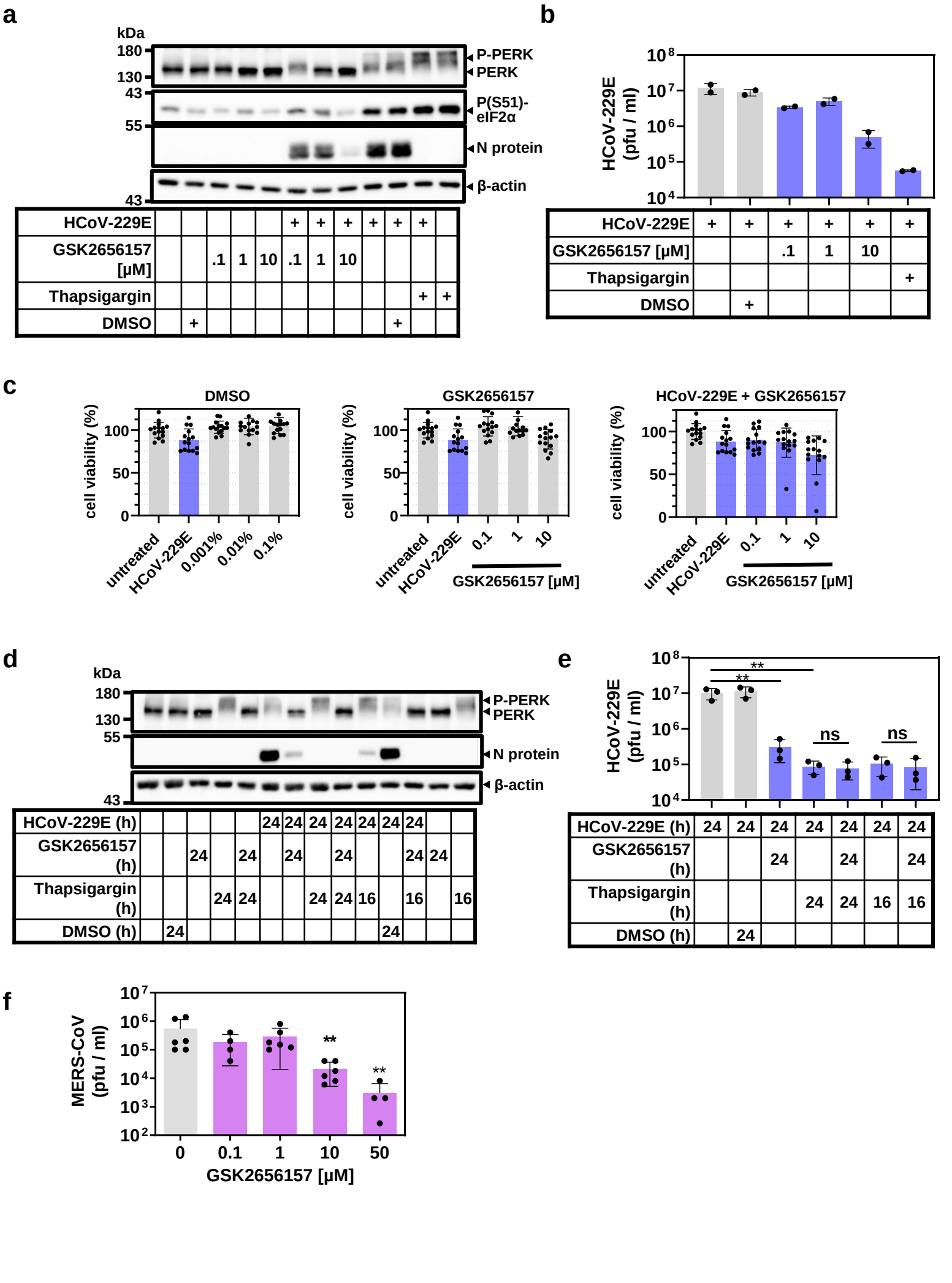
a
kDa
180
130
43
55
43
P-PERK
PERK
P(S51)-eIF2α
N protein
β-actin
HCoV-229E + + + + + + + + + + + +
GSK2656157 [μM] .1 1 10 .1 1 10
Thapsigargin + +
DMSO + +
b
HCoV-229E (pfu / ml)
HCoV-229E + + + + + +
GSK2656157 [μM] .1 1 10
Thapsigargin +
DMSO +
c
DMSO
GSK2656157
HCoV-229E + GSK2656157
cell viability (%)
untreated
HCoV-229E
0.001%
0.01%
0.1%
0.1
1
10
GSK2656157 [μM]
d
kDa
180
130
55
43
P-PERK
PERK
N protein
β-actin
HCoV-229E (h) 24 24 24 24 24 24 24
GSK2656157 (h) 24 24 24 24 24
Thapsigargin (h) 24 24 24 24 16 16 16
DMSO (h) 24 24
e
HCoV-229E (pfu / ml)
**
**
ns
ns
HCoV-229E (h) 24 24 24 24 24 24 24
GSK2656157 (h) 24 24 24 24
Thapsigargin (h) 24 24 16 16
DMSO (h) 24
f
MERS-CoV (pfu / ml)
**
**
0
0.1
1
10
50
GSK2656157 [μM]

Supplementary Fig. 2. PERK inhibition by GSK2656157 suppresses CoV replication.
(a) HuH7 cells were pretreated with increasing concentrations of the PERK inhibitor GSK2656157 for 30 min or with solvent (DMSO), or were left untreated. Then, cells were infected with HCoV-229E (MOI = 1) as indicated. Cell extracts were analyzed by immunoblotting for the phosphorylation or expression of the indicated proteins (one representative out of two independent experiments).
(b) Viral titers in supernatants obtained from cells treated or infected as in (a) (two biologically independent experiments).
(c) Cell viabilities (by MTS assays) of cells treated as in (a). Data points show replicate determinations of five independent experiments.
(d, e) HuH7 cells were infected and treated with the indicated combinations of GSK2656157 (10 μM) and thapsigargin (1 μM). Activation or suppression of PERK and N protein levels were determined by immunoblotting of cell extracts. (d) shows one out of two representative immunoblot experiment, (e) shows viral titers of supernatants (three biologically independent experiments).
(f) Viral titers of supernatants from HuH7 cells infected with MERS-CoV in the presence or absence of increasing concentrations of GSK2656157 (four or more biologically independent experiments).
All bar graphs show means ± s.d.; asterisks indicate p values (* $p \leq 0.05$, ** $p \leq 0.01$, *** $p \leq 0.001$, **** $p \leq 0.0001$) obtained by two-tailed unpaired t-tests (e) or Mann Withney tests (f).

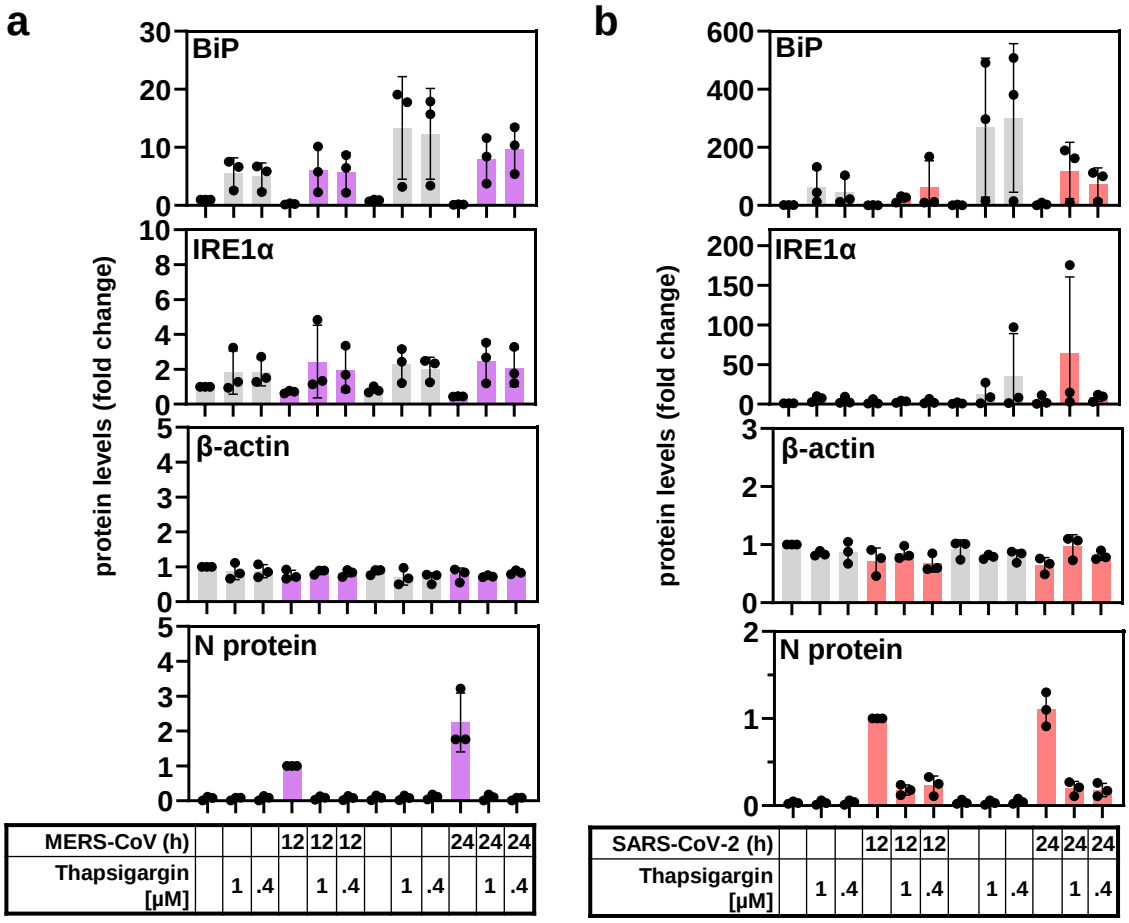
a
b
BiP
IRE1α
β-actin
N protein
protein levels (fold change)
MERS-CoV (h)
SARS-CoV-2 (h)
Thapsigargin [μM]
12
24
1
.4

Supplementary Fig. 3. Thapsigargin suppresses MERS-CoV and SARS-CoV-2 N protein and upregulates BiP in infected cells.
(a, b) show the quantification of replicate immunoblot experiments performed as shown in Fig. 4g and 4h. All bar graphs show means ± s.d. (three biologically independent experiments).

a

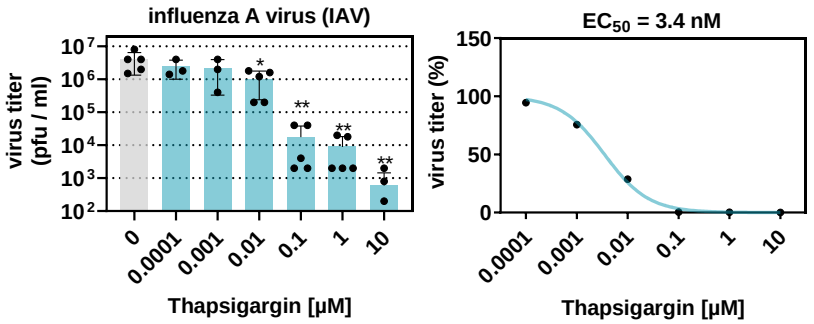
influenza A virus (IAV)
virus titer (pfu / ml)
10^7
10^6
10^5
10^4
10^3
10^2
*
**
**
0
0.0001
0.001
0.01
0.1
1
10
Thapsigargin [µM]
EC_{50} = 3.4 nM
virus titer (%)
150
100
50
0
0.0001
0.001
0.01
0.1
1
10
Thapsigargin [µM]

b

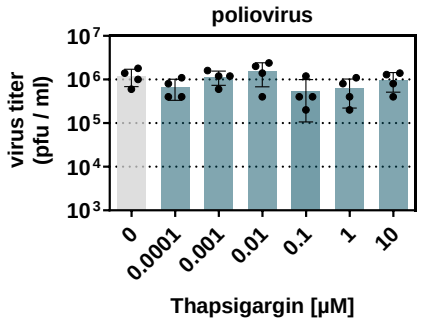
poliovirus
virus titer (pfu / ml)
10^7
10^6
10^5
10^4
10^3
0
0.0001
0.001
0.01
0.1
1
10
Thapsigargin [µM]

Supplementary Fig. 4. Thapsigargin suppresses Influenza A virus but not poliovirus replication.
(a) Shown are viral titers and the EC_{50} (for IAV) of A549 cells infected with IAV virus (strain A/Thailand/1(KAN-1)/2004, H5N1) at an MOI of 0.01 for 24 h (three or more biologically independent experiments).
(b) Viral titers of Vero E6 cells infected with poliovirus at an MOI of 0.1 for 24 h and treated with thapsigargin as indicated (four biologically independent experiments).
All bar graphs show means ± s.d.; asterisks indicate p values (* $p \leq 0.05$, ** $p \leq 0.01$, *** $p \leq 0.001$, **** $p \leq 0.0001$) obtained by two-tailed unpaired t-tests.

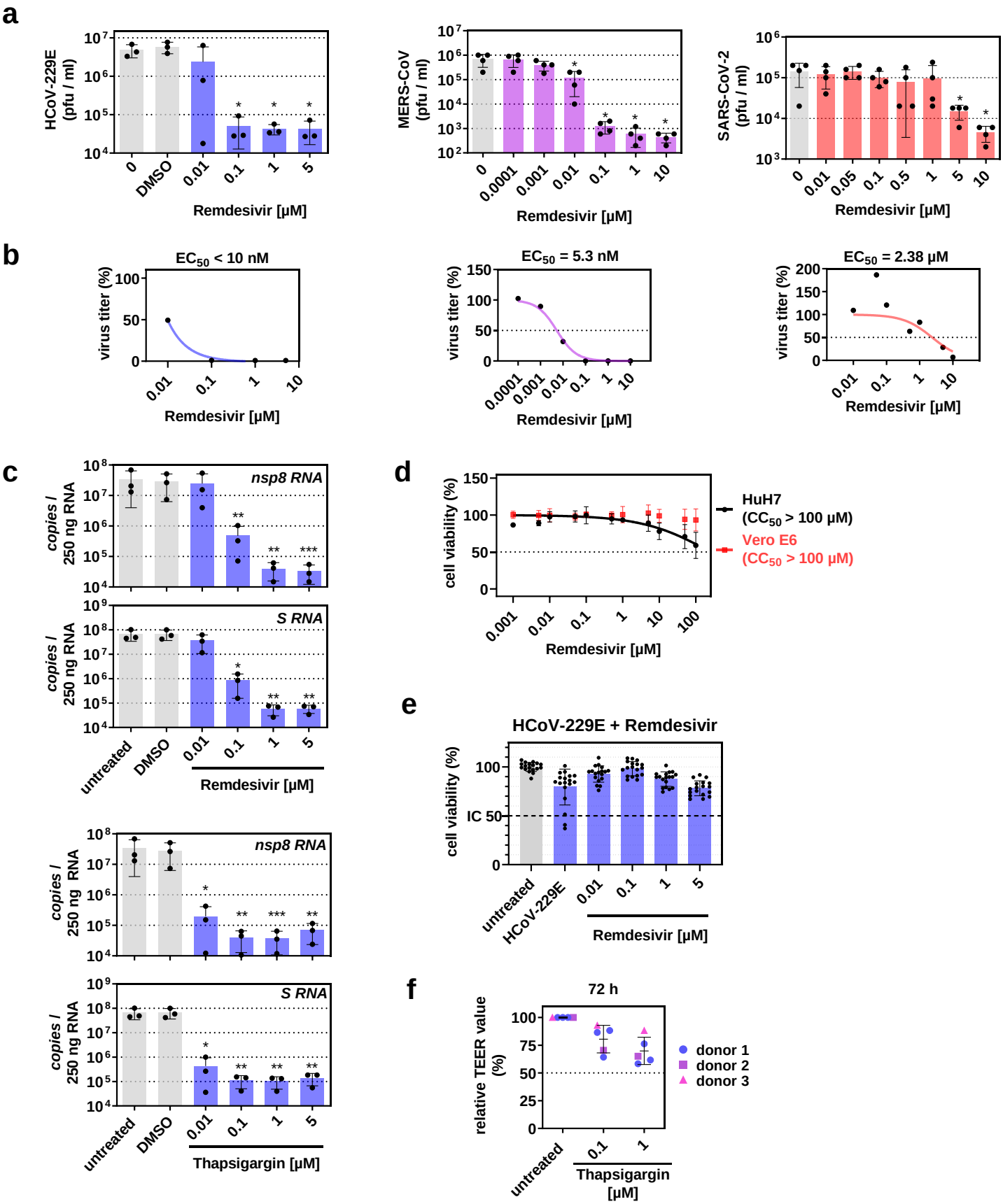
a
HCoV-229E (pfu / ml)
Remdesivir [µM]
0
DMSO
0.01
0.1
1
5
MERS-CoV (pfu / ml)
0.0001
0.001
10
SARS-CoV-2 (pfu / ml)
0.05
0.5
b
EC50 < 10 nM
virus titer (%)
EC50 = 5.3 nM
EC50 = 2.38 µM
c
nsp8 RNA
S RNA
copies / 250 ng RNA
untreated
Thapsigargin [µM]
d
cell viability (%)
HuH7
(CC50 > 100 µM)
Vero E6
(CC50 > 100 µM)
e
HCoV-229E + Remdesivir
IC 50
f
72 h
relative TEER value (%)
donor 1
donor 2
donor 3

Supplementary Fig. 5. Comparison of the antiviral effects of thapsigargin and remdesivir.
(a, b) HuH7 cells infected with HCoV-229E (MOI of 1) or MERS-CoV (MOI of 0.5) or Vero E6 cells infected with SARS-CoV-2 (MOI of 0.5) for 24 h with an were treated with increasing concentrations of remdesivir and viral titers in the supernatants obtained from these cells (a) were used to calculate the EC_{50} values shown in (b). Data represent three (HCoV-229E) or four (MERS-CoV, SARS-CoV-2) biologically independent experiments.
(c) Direct comparison of the effects of remdesivir or thapsigargin on the synthesis of viral RNAs in cells infected with HCoV-229E as described in (a) (three biologically independent experiments).
(d) Cytotoxicity of remdesivir in untreated HuH7 or Vero E6 cells. Data show CC_{50} estimations obtained from two or more biologically independent experiments.
(e) Cytotoxicity of remdesivir in HuH7 cells infected with HCoV-229E (24 h, MOI of 1) as determined by MTS assays. Data points show replicate determinations representing six biologically independent experiments.
(f) Viability of differentiated NHBE cells treated for 72 h with two doses of thapsigargin was compared to untreated cells by TEER assay (three biologically independent experiments).
All bar graphs show means ± s.d.; asterisks indicate p values (* $p \leq 0.05$, ** $p \leq 0.01$, *** $p \leq 0.001$, **** $p \leq 0.0001$) obtained by two-tailed unpaired t-tests.

12 h MERS-CoV

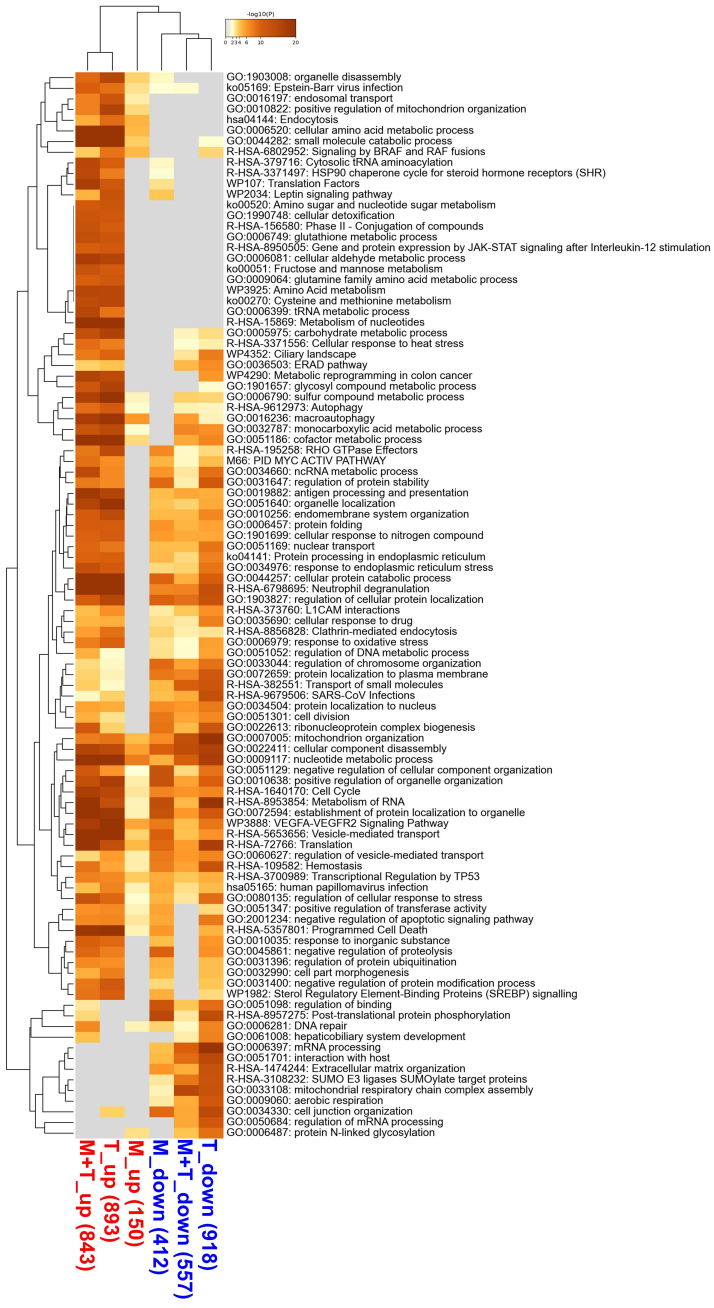

24 h MERS-CoV

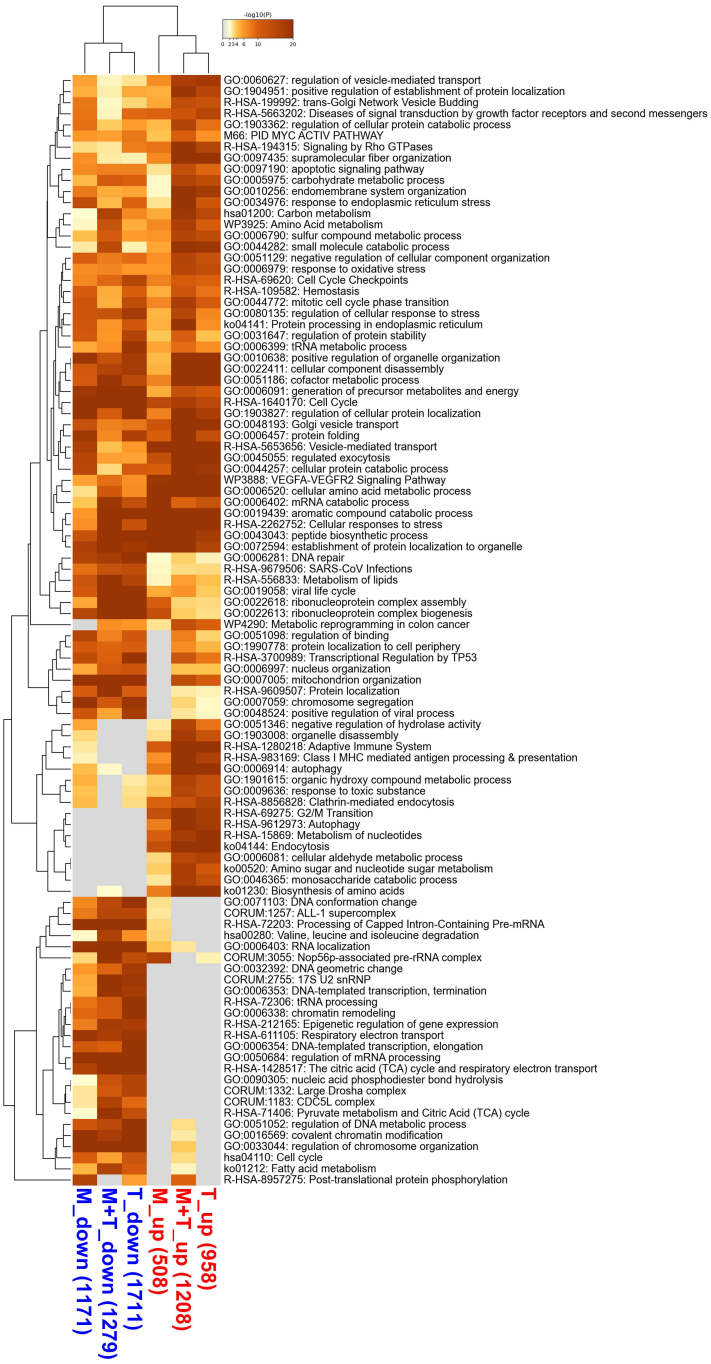

Supplementary Fig. 6. Identification of deregulated cellular pathways in MERS-CoV-infected HuH7 cells.

Top 100 overrepresented pathways containing up- or downregulated DEPs (ratio > 0, p value of $-\log_{10}(p) \geq 1.3$) for the 12 h p.i. and 24 h p.i. time points of MERS-CoV-infected cells based on gene IDs derived from protein IDs. Blue and red colors indicate differentially expressed proteins as shown in Fig. 6a, b, e. See the legends of Fig. 6 and Methods for details.

12 h SARS-CoV-2

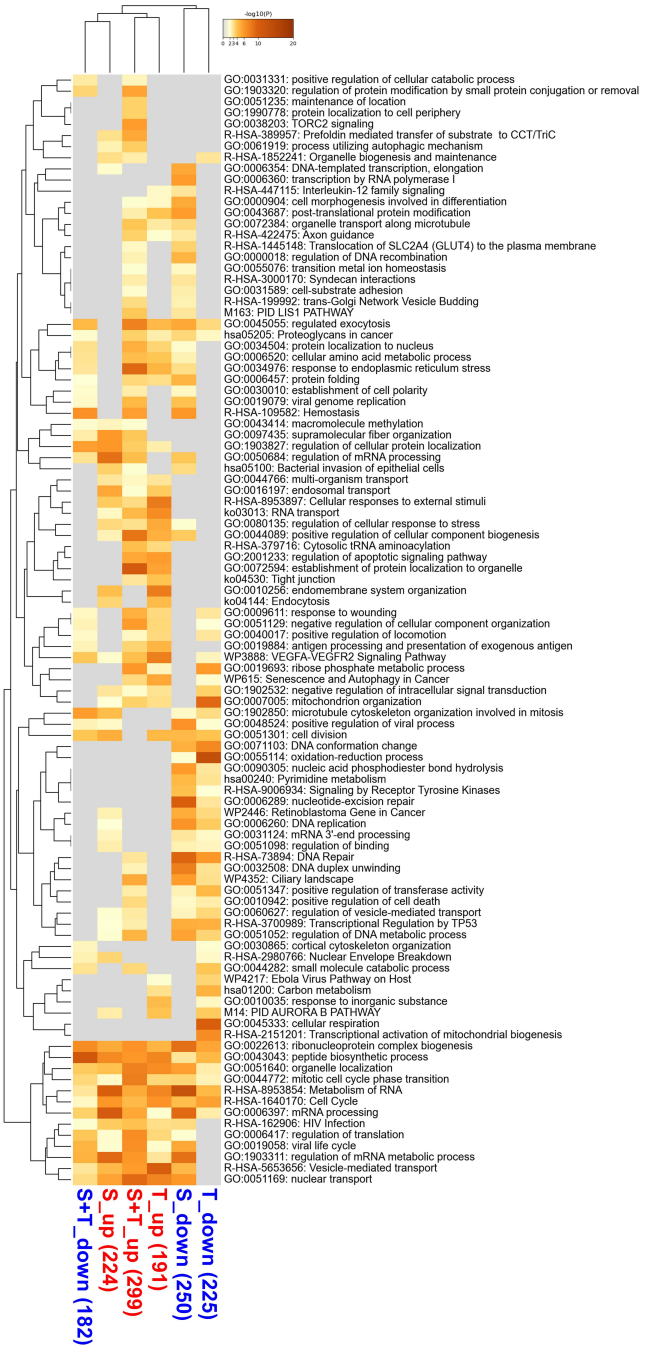

24 h SARS-CoV-2

Supplementary Fig. 7. Identification of deregulated cellular pathways in SARS-CoV-2-infected Vero E6 cells.

Top 100 overrepresented pathways containing up- or downregulated DEPs (ratio > 0, p value of $-\log_{10}(p) \geq 1.3$) for the 12 h p.i. and 24 h p.i. time points of SARS-CoV-2-CoV-infected cells based on gene IDs derived from protein IDs. Blue and red colors indicate differentially expressed proteins as shown in Fig. 6c, d, e. See the legends of Fig. 6 and Methods for details.

a

condition	time	GO	description	DEPs↑	DEPs↓
MERS-CoV	12h	GO:0009117	nucleotide metabolic process	-7.9	-5.0
		GO:0016236	macroautophagy	-5.9	
		GO:0022411	cellular component disassembly	-5.7	-10.1
		WP3888	VEGFA-VEGFR2 Signaling Pathway	-5.4	-8.1
		hsa04144	Endocytosis	-4.8	
		R-HSA-8957275	Post-translational protein phosphorylation		-14.8
		R-HSA-8953854	Metabolism of RNA		-13.9
		GO:0051129	negative regulation of cellular component organization		-13.0
		GO:0072594	establishment of protein localization to organelle		-13.0
		GO:0010638	positive regulation of organelle organization		-12.8
MERS-CoV	24h	R-HSA-2262752	Cellular responses to stress	-33.4	-6.6
		GO:0043043	peptide biosynthetic process	-32.5	-13.0
		GO:0006402	mRNA catabolic process	-28.7	-3.9
		GO:0019439	aromatic compound catabolic process	-27.2	-6.2
		GO:0006520	cellular amino acid metabolic process	-22.8	-3.2
		R-HSA-72203	Processing of Capped Intron-Containing Pre-mRNA	-3.3	-32.5
		GO:1903827	regulation of cellular protein localization	-7.7	-24.2
		GO:0050684	regulation of mRNA processing		-24.1
		R-HSA-1640170	Cell Cycle	-14.8	-23.6
		GO:0007005	mitochondrion organization		-22.6
SARS-CoV-2	12h	GO:0006397	mRNA processing	-11.0	-9.2
		R-HSA-8953854	Metabolism of RNA	-10.1	-12.7
		GO:1903311	regulation of mRNA metabolic process	-9.2	-8.7
		GO:0050684	regulation of mRNA processing	-8.7	-3.9
		GO:0043043	peptide biosynthetic process	-7.0	
		R-HSA-8953854	Metabolism of RNA	-10.1	-12.7
		GO:0006289	nucleotide-excision repair		-10.0
		R-HSA-73894	DNA Repair		-9.6
		GO:0006397	mRNA processing	-11.0	-9.2
		GO:0022613	ribonucleoprotein complex biogenesis	-5.2	-9.0
SARS-CoV-2	24h	GO:0086073	..His cell-Purkinje myocyte adhesion in communication	-6.83	
		GO:1903827	regulation of cellular protein localization	-5.9	-6.3
		R-HSA-5653656	Vesicle-mediated transport	-5.2	-4.6
		GO:0097435	supramolecular fiber organization	-5.0	
		GO:0090407	organophosphate biosynthetic process	-4.19	
		GO:0043687	post-translational protein modification		-10.5
		R-HSA-8953854	Metabolism of RNA		-10.0
		R-HSA-8957275	Post-translational protein phosphorylation		-7.2
		R-HSA-5696398	Nucleotide Excision Repair		-7.1
		R-HSA-69278	Cell Cycle, Mitotic		-7.0
Thapsigargin HuH7	12h	GO:0006520	cellular amino acid metabolic process	-49.0	
		GO:0051186	cofactor metabolic process	-43.3	-7.2
		R-HSA-5653656	Vesicle-mediated transport	-42.7	-6.4
		GO:0009117	nucleotide metabolic process	-38.9	-17.5
		R-HSA-5357801	Programmed Cell Death	-28.9	-4.8
		GO:0006397	mRNA processing		-24.7
		R-HSA-8953854	Metabolism of RNA	-13.7	-23.7
		GO:0007005	mitochondrion organization	-8.5	-20.5
		R-HSA-72766	Translation	-13.5	-17.5
		GO:0009117	nucleotide metabolic process	-38.9	-17.5
Thapsigargin HuH7	24h	R-HSA-5653656	Vesicle-mediated transport	-59.1	-6.0
		GO:0006520	cellular amino acid metabolic process	-34.5	-6.8
		GO:0051186	cofactor metabolic process	-34.5	-14.7
		ko04144	Endocytosis	-31.1	
		WP3888	VEGFA-VEGFR2 Signaling Pathway	-30.9	-6.7
		R-HSA-72203	Processing of Capped Intron-Containing Pre-mRNA		-100.0
		GO:0022613	ribonucleoprotein complex biogenesis	-3.1	-71.0
		GO:0006403	RNA localization		-49.6
		GO:0050684	regulation of mRNA processing		-46.6
		R-HSA-1640170	Cell Cycle	-14.9	-40.6
Thapsigargin Vero E6	12h	R-HSA-5653656	Vesicle-mediated transport	-10.4	
		R-HSA-8953897	Cellular responses to external stimuli	-8.1	
		GO:0010256	endomembrane system organization	-8.0	
		WP3888	VEGFA-VEGFR2 Signaling Pathway	-7.8	
		GO:0051169	nuclear transport	-7.4	
		GO:0055114	oxidation-reduction process		-13.5
		GO:0045333	cellular respiration		-10.2
		GO:0007005	mitochondrion organization	-3.1	-9.4
		GO:0071103	DNA conformation change		-7.1
		R-HSA-2151201	Transcriptional activation of mitochondrial biogenesis		-6.9
Thapsigargin Vero E6	24h	GO:0034976	response to endoplasmic reticulum stress	-11.3	
		ko00520	Amino sugar and nucleotide sugar metabolism	-9.8	
		WP3888	VEGFA-VEGFR2 Signaling Pathway	-8.9	
		R-HSA-8957275	Post-translational protein phosphorylation	-8.2	
		GO:0072594	establishment of protein localization to organelle	-8.2	
		R-HSA-69278	Cell Cycle, Mitotic		-11.9
		GO:0009141	nucleoside triphosphate metabolic process		-10.2
		GO:0051301	cell division		-7.44
		R-HSA-2980766	Nuclear Envelope Breakdown		-6.9
		WP4932	7q11.23 copy number variation syndrome		-6.1

top10 pathways

- DNA
- RNA
- metabolism
- localization

enrichment $\log_{10}$ p value

0 -20

b

	GO	description	virus DEPs↑	virus DEPs↓	Thapsigargin DEPs↑	Thapsigargin DEPs↓
Thapsigargin (52)	GO:1901657	glycosyl compound metabolic process			-16.7	
	ko00270	Cysteine and methionine metabolism			-15.2	
	GO:0032787	monocarboxylic acid metabolic process			-14.7	-6.7
	GO:0046365	monosaccharide catabolic process			-13.5	
	GO:0006749	glutathione metabolic process			-12.1	
	GO:0009064	glutamine family amino acid metabolic process			-11.7	
	GO:1990748	cellular detoxification			-11.5	
	R-HSA-8950505	.JAK-STAT signaling after Interleukin-12 stimulation			-11.4	
	ko00051	Fructose and mannose metabolism			-11.0	
	R-HSA-156580	Phase II - Conjugation of compounds			-10.5	
	CORUM:1332	Large Drosha complex				-15.9
	R-HSA-71406	Pyruvate metabolism and Citric Acid (TCA) cycle				-13.6
	GO:0055114	oxidation-reduction process				-13.5
	GO:0033108	mitochondrial respiratory chain complex assembly				-12.9
	R-HSA-3108232	SUMO E3 ligases SUMOylate target proteins				-12.6
	GO:0009060	aerobic respiration				-11.5
	GO:0009141	nucleoside triphosphate metabolic process				-10.2
	GO:0045333	cellular respiration				-10.2
	CORUM:1183	CDC5L complex				-9.3
	GO:0061008	hepaticobiliary system development				-7.5

			virus DEPs↑	virus DEPs↓	Thapsigargin DEPs↑	Thapsigargin DEPs↓
Thapsigargin, MERS-CoV, SARS-CoV-2 (36)	R-HSA-2262752	Cellular responses to stress	-33.4	-6.6	-24.6	-12.8
	GO:0043043	peptide biosynthetic process	-32.5	-13.0	-17.8	-30.4
	R-HSA-5653656	Vesicle-mediated transport	-20.2	-17.1	-59.1	-6.0
	R-HSA-1640170	Cell Cycle	-14.8	-23.6	-14.9	-40.6
	GO:0045055	regulated exocytosis	-13.5	-15.3	-20.2	-5.5
	GO:0022613	ribonucleoprotein complex biogenesis	-13.4	-15.5	-3.1	-71.0
	ko04144	Endocytosis	-13.4		-31.1	
	GO:0006397	mRNA processing	-11.0	-9.2		
	GO:0044257	cellular protein catabolic process	-10.3	-15.2	-19.0	-11.1
	GO:0006457	protein folding	-10.3	-18.7	-13.4	-17.0
	GO:1903827	regulation of cellular protein localization	-7.7	-24.2	-17.3	-20.1
	GO:0050684	regulation of mRNA processing		-24.1		-46.6
	R-HSA-1640170	Cell Cycle	-14.8	-23.6	-14.9	-40.6
	GO:0007005	mitochondrion organization		-22.6	-11.0	-27.1
	GO:0006457	protein folding	-10.3	-18.7	-13.4	-17.0
	R-HSA-5653656	Vesicle-mediated transport	-20.2	-17.1	-59.1	-6.0
	R-HSA-8957275	Post-translational protein phosphorylation		-16.3		-5.7
	GO:0022613	ribonucleoprotein complex biogenesis	-13.4	-15.5	-3.1	-71.0
	GO:0045055	regulated exocytosis	-13.5	-15.3	-20.2	-5.5
	GO:0044257	cellular protein catabolic process	-10.3	-15.2	-19.0	-11.1

enrichment $\log_{10}$ p value

0 -20

Supplementary Fig. 8. Top pathways regulated by MERS-CoV, SARS-CoV-2 or thapsigargin.
(a) Top ten enriched pathways containing up- or downregulated DEPs extracted from the 100 enriched deregulated pathways shown in Fig. S6 / Fig. S7. Colors indicate highly common categories.
(b) Top 20 pathways enriched with thapsigargin alone or jointly by MERS-CoV, SARS-CoV-2 and thapsigargin according to the Venn diagram shown in Fig. 6f. See the legends of Fig. 6 and Methods for details.

Pathway KEGG: hsa04141

MERS-CoV / - (24 h)

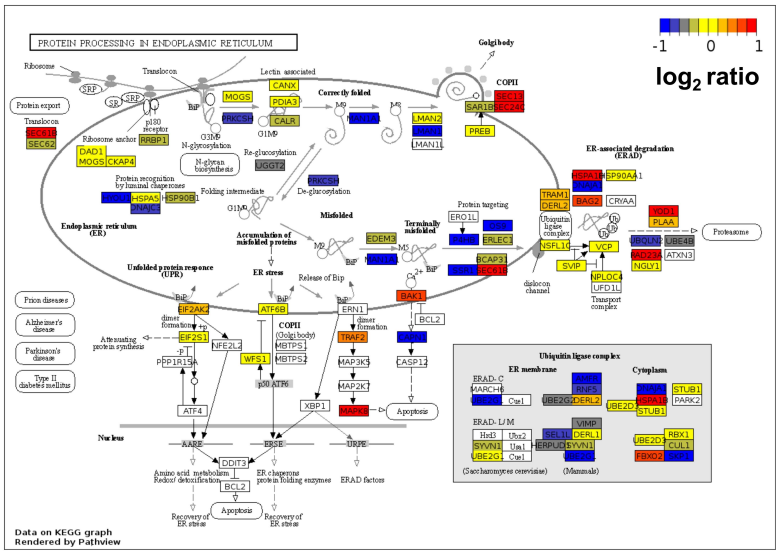

MERS-CoV + Thapsigargin / MERS-CoV (24 h)

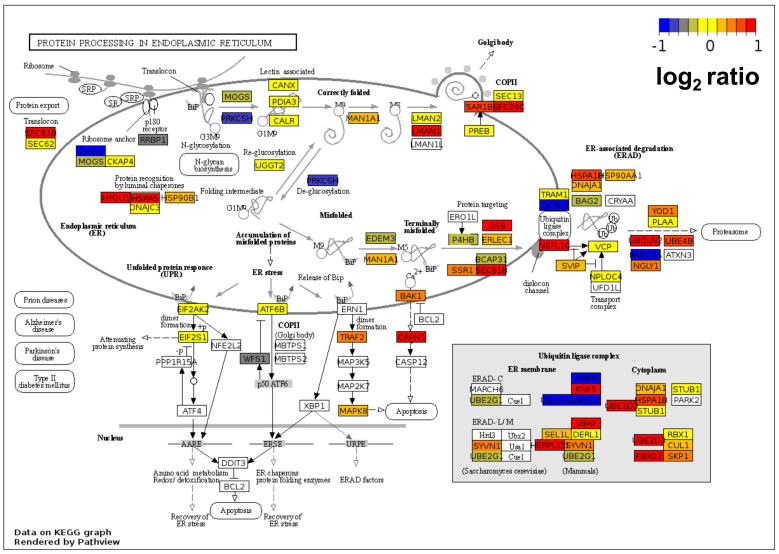

SARS-CoV-2 / - (24 h)

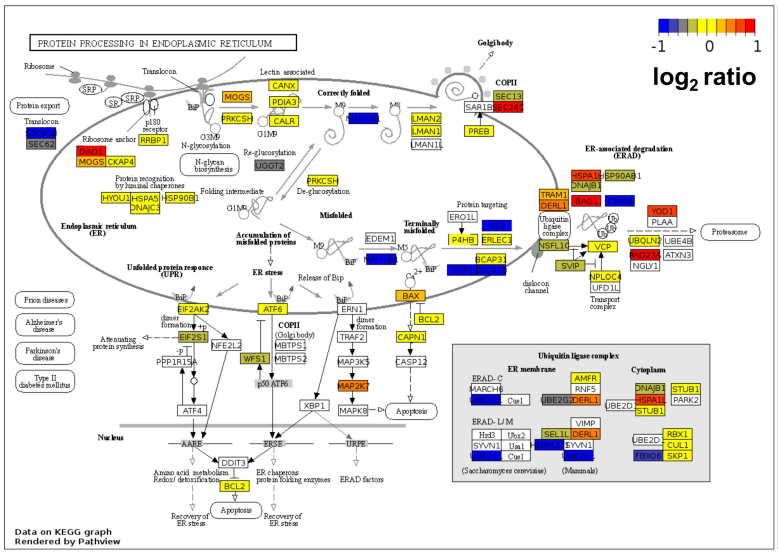

SARS-CoV-2 + Thapsigargin / SARS-CoV-2 (24 h)

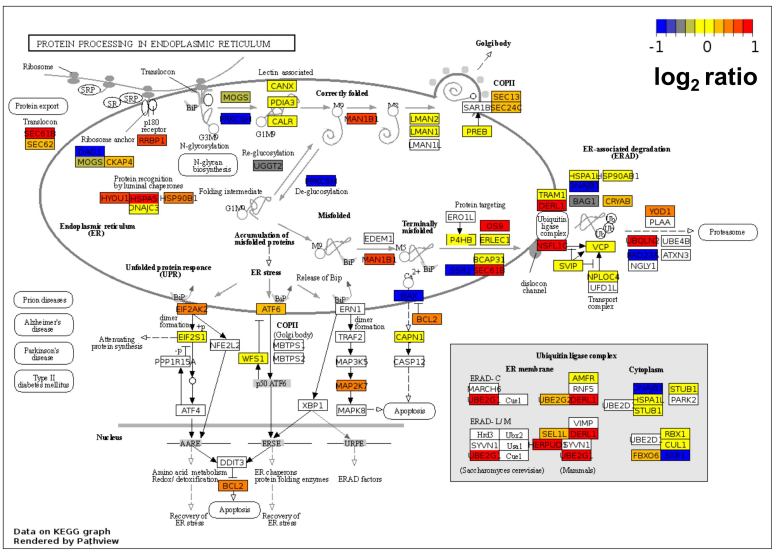

Supplementary Fig. 9. Projection of thapsigargin effects on protein levels of pathway KEGG hsa04141.

Mean ratio values of all pathway components measured by LC-MS/MS in untreated cells and 24 h p.i. were projected on the KEGG hsa04141 pathway map (left graphs). The right graphs show the corresponding changes imposed by thapsigargin treatment of infected cells.

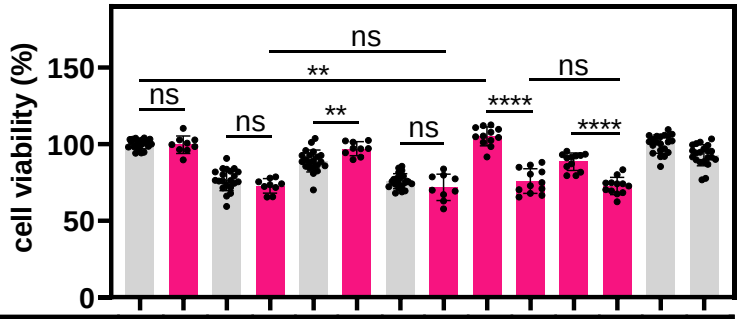

	1	2	3	4	5	6	7	8	9	10	11	12	13	14
HCoV-229E (24 h)					+	+	+	+			+	+		+
Bafilomycin A_1 (h)		28		28		28		28	16	16	16	16		
Thapsigargin (24 h)			+	+			+	+		+		+		
DMSO (28 h)													+	+

Supplementary Fig. 10. Effects of bafilomycin A_1 on the viability of HCoV-229E-infected and thapsigargin-treated HuH7 cells.

Experiments were performed as described in the legend of Fig. 8. Cell viability was determined by MTS assay. Data points show replicate determinations representing three (28 h bafilomycin A_1 treatment conditions) or four (16 h bafilomycin A_1 treatment conditions) biologically independent experiments. The bar graph shows means ± s.d.; asterisks indicate p values (* $p \leq 0.05$, ** $p \leq 0.01$, *** $p \leq 0.001$, **** $p \leq 0.0001$) obtained by two-tailed unpaired t-tests.

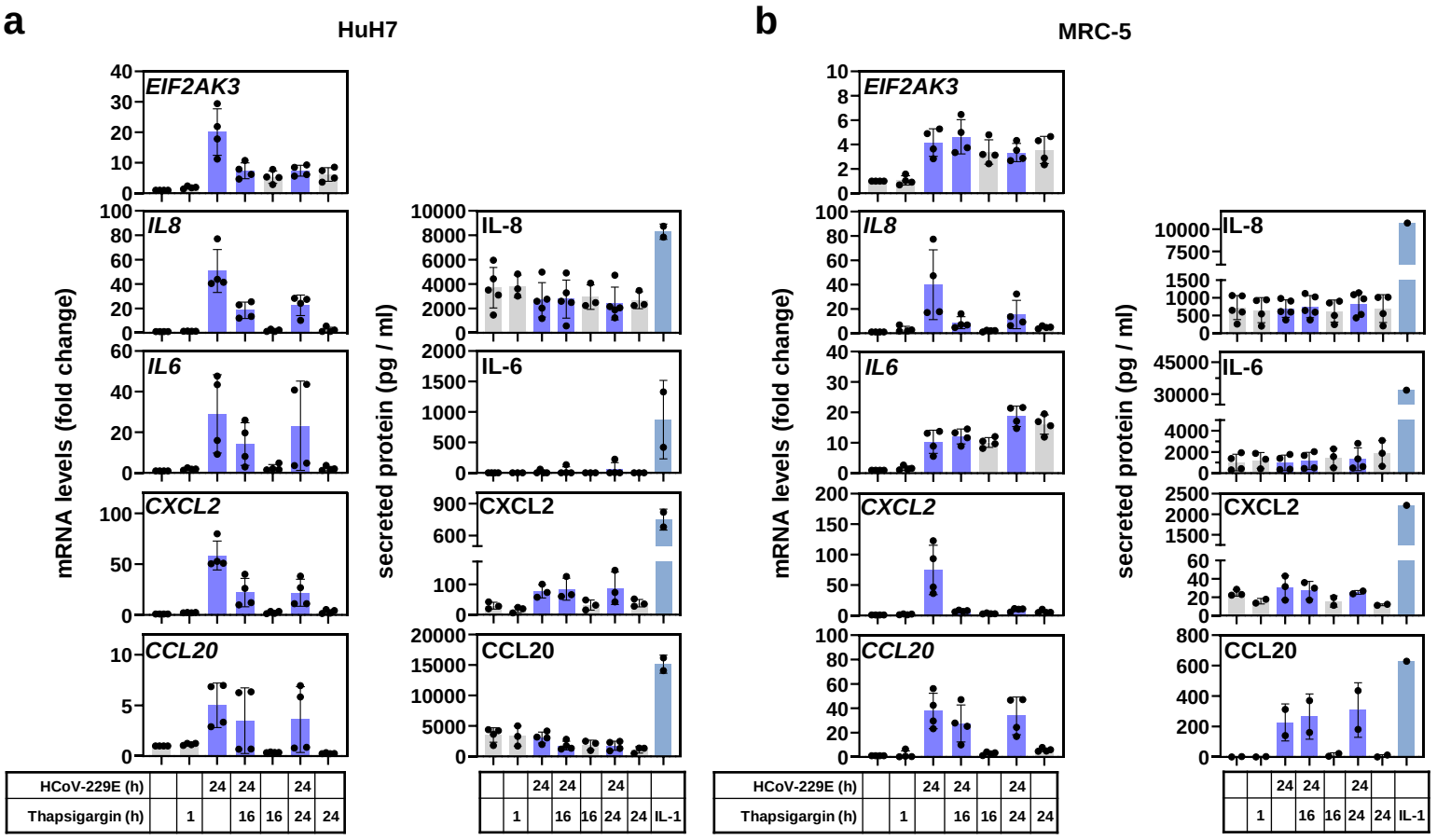
a
HuH7
b
MRC-5
mRNA levels (fold change)
secreted protein (pg / ml)
EIF2AK3
IL8
IL6
CXCL2
CCL20
IL-8
IL-6
IL-1
HCoV-229E (h)
Thapsigargin (h)

Supplementary Fig. 11. Analysis of inflammatory host cell transcripts showing thapsigargin-independent uncoupling of mRNA and protein levels in HCoV-229E-infected cells.
HuH7 (a) or MRC-5 (b) cells were infected as described in Fig. 2b. Total RNA was used to analyze expression of inflammatory transcripts by RT-qPCR (left graphs) and the secretion of the corresponding proteins by ELISA (right graphs). Additionally, expression of the *EIF2AK3* mRNA encoding the PERK protein kinase was determined. PERK protein levels of HuH7 cells are shown in Fig. 2e-f. All bar graphs show means ± s.d.. Data points show individual values from two or more biologically independent experiments with the exception of IL-1 treatments which were used as positive controls for one or two experiments as indicated.

Table 1: Commercial Taqman assays used for RT-qPCR

transcript	length of PCR product (bp)	assay ID	source
GUSB	81	Hs99999908_m1	Applied Biosystems / Thermo Fisher Scientific
IL6	95	Hs00174131_m1	Applied Biosystems / Thermo Fisher Scientific
IL8 (CXCL8)	101	Hs00174103_m1	Applied Biosystems / Thermo Fisher Scientific
CXCL2	68	Hs00236966_m1	Applied Biosystems / Thermo Fisher Scientific
CCL20	81	Hs00171125_m1	Applied Biosystems / Thermo Fisher Scientific

Table 2: Additional primers designed for RT-qPCR

transcript	forward sequence	reverse sequence
EIF2AK3	5'-AGAGATTGAGACTGCGTGGC-3'	5'-TCCCAAATACCTCTGGTTTGCT-3'
HCoV-229E S RNA	5‘-TTTCAGGTGATGCTCACATACC-3‘	5‘-ACAAACTCACGAACTGTCTTAGG-3‘
HCoV-229E nsp8 RNA	5‘-GCTGTTGCAAATGGTTCCTCAC-3‘	5‘-GATGCACATTCTTACCATCATTATCC-3‘

Supplementary Table 1. List of all commercial Taqman assays and primers used in this study.